ResearchGate

See discussions, stats, and author profiles for this publication at: https://www.researchgate.net/publication/261117033

Automatic cerebral aneurysm detection in multimodal angiographic images

Conference Paper · October 2011

DOI: 10.1109/NSSMIC.2011.6152566

CITATIONS
21

READS
229

4 authors, including:

Oliver Beuing
University Hospital Magdeburg
112 PUBLICATIONS **1,227** CITATIONS
SEE PROFILE

Rosa Nickl
Universitätsklinikum Carl Gustav Carus Dresden
5 PUBLICATIONS **52** CITATIONS
SEE PROFILE

Klaus D Tönnies
Otto-von-Guericke-Universität Magdeburg
253 PUBLICATIONS **1,826** CITATIONS
SEE PROFILE

Some of the authors of this publication are also working on these related projects:

Computer Assisted Intervention View project

Intravascular Assessment, Visualization and Evaluation of the Cerebral Vessel Wall View project

All content following this page was uploaded by Oliver Beuing on 02 July 2014.

The user has requested enhancement of the downloaded file.

Automatic Cerebral Aneurysm Detection in Multimodal Angiographic Images

Clemens M. Hentschke, Oliver Beuing, Rosa Nickl and Klaus D. Tönnies

***Abstract*—We propose a system to automatically detect cerebral aneurysms in 3D X-ray rotational angiography (3D-RA) images, magnetic resonance angiography (MRA) images and computed tomography angiography (CTA) images. The aneurysms are found by analyzing a blob-enhancing filtered image. Our method was tested on 65 angiographic data sets. The features leading to the best discrimination between false positives (FP) and aneurysms were identified. We achieved 96 % sensitivity with an average rate of 2.6 FP per data set in case of 3D-RA, 94 % sensitivity with an average rate of 8.0 FP per data set in case of MRA and 90 % sensitivity with an average rate of 28.1 FP per data set with CTA, respectively.**

***Index Terms*—Computer Aided Diagnosis, Cerebral Aneurysm detection, Angiography.**

I. Introduction

Between 3.6 % and 6 % of the population harbors one or more cerebral aneurysms [1]. Cerebral aneurysms are subject to rupture leading to life-threatening subarachnoid hemorrhage. The mortality rate for this pathology is reported to be approximately 50 % while 46 % of the survivors have long-time impairments [2], [3]. Prognosis if and when an aneurysm ruptures is currently only possible with insufficient accuracy. Rupture of aneurysms has to be prevented with respect to clinical and economical aspects. Hence, early finding of cerebral aneurysms is desirable.

Image modalities that are clinically relevant in aneurysm detection are 2D digital subtraction angiography (2D-DSA), 3D X-ray rotational angiography (3D-RA, Fig. 1(a)), magnetic resonance angiography (MRA, Fig. 1(b)) and computed tomography angiography (CTA, Fig. 1(c)). Cerebral aneurysms are commonly found incidentally in these angiographic images as they are used for detection and therapy of cerebrovascular diseases. In this paper, we focus on the three-dimensional modalities.

Only few methods have been proposed to detect cerebral aneurysms in medical images [4], [5], [6], [7]. All algorithms rely on a two-step strategy that first detects candidate regions and then examines these regions for their probability being an aneurysm. Three different strategies are used for initial findings: shape-based, skeleton-based and difference image based approaches. Shape-based algorithms rely on the assumption that aneurysms are sphere-shaped [6]. Skeleton-based systems aim at finding terminating branches in the skeleton of a data set representing the vessel structure [4]. Difference image approaches use a subtraction of a normal vessel model from the original data set to find suspicious regions [5]. Hybrid approaches that use a combination of two or more methods also exist [4], [7]. The second step aims at reducing the amount of false positives (FP) based on classification by linear or quadratic discriminant analysis [4], rule-based systems [7] or case-based reasoning [5]. All proposed algorithms are intended to work with MRA data sets except [6], which implements a multi-modal approach on 3D-RA and CTA data sets. A prerequisite of all methods is a segmentation of the vasculature that heavily influences the detection quality.

If automatic aneurysm detection should be useful in clinical routine, it needs to be part of a Computer Aided Diagnosis scheme that is adaptable to all of the three-dimensional modalities mentioned above. However, many approaches neglect the clinical applicability by incorporating restrictive requirements like a segmented vasculature, various parameters and a large prototypic image database for training. In contrast, we propose a general approach that works on multimodal angiographic images with minimal preprocessing.

II. Method

Our workflow consists of four parts that is the same for all modalities except for the parametrization (Fig. 2):

1) The 3D-RA, MRA and CTA data sets are normalized.
2) Initial regions of potential aneurysms are found by a filter that enhances spherical structures (blobness filter).
3) Volumes of Interest (VOI) are found by applying a modified k-means clustering on the filtered image.
4) Each VOI is analyzed in a post-processing step based on a rule-based system and a thresholding of a suitable feature.

In step 1, the images are intensity normalized to [0, 2048] and orientation normalized, such that the (x/y/z) coordinates of the image correspond to left-right direction, to anterior-posterior direction and superior-inferior direction, respectively. CTA data sets are already intensity normalized due to HU. If necessary, the images are resampled to isotropic voxel size by linear interpolation. No segmentation is required.

Initial aneurysm candidates are found by enhancing the original image by a multi-scale sphere-enhancing filter (step 2,

Manuscript received November 15, 2011. This work was supported in part by the DFG (research grant TO166/13-1).

C. M. Hentschke is with the Department of Simulation and Graphics, University of Magdeburg, Magdeburg, Germany (telephone: +49 391 67 11441, e-mail: clemens.hentschke@ovgu.de).

O. Beuing is with the Institute of Neuroradiology, University Hospital of Magdeburg, Magdeburg, Germany (telephone: +49 391 67 21681, e-mail: oliver.beuing@med.ovgu.de).

R. Nickl is with the Institute of Neuroradiology, University Hospital of Magdeburg, Magdeburg, Germany (telephone: +49 391 67 21681, e-mail: rosanickl@gmx.de).

K. D. Tönnies is with the Department of Simulation and Graphics, University of Magdeburg, Magdeburg, Germany (telephone: +49 391 67 18772 , e-mail: klaus.toennies@ovgu.de).

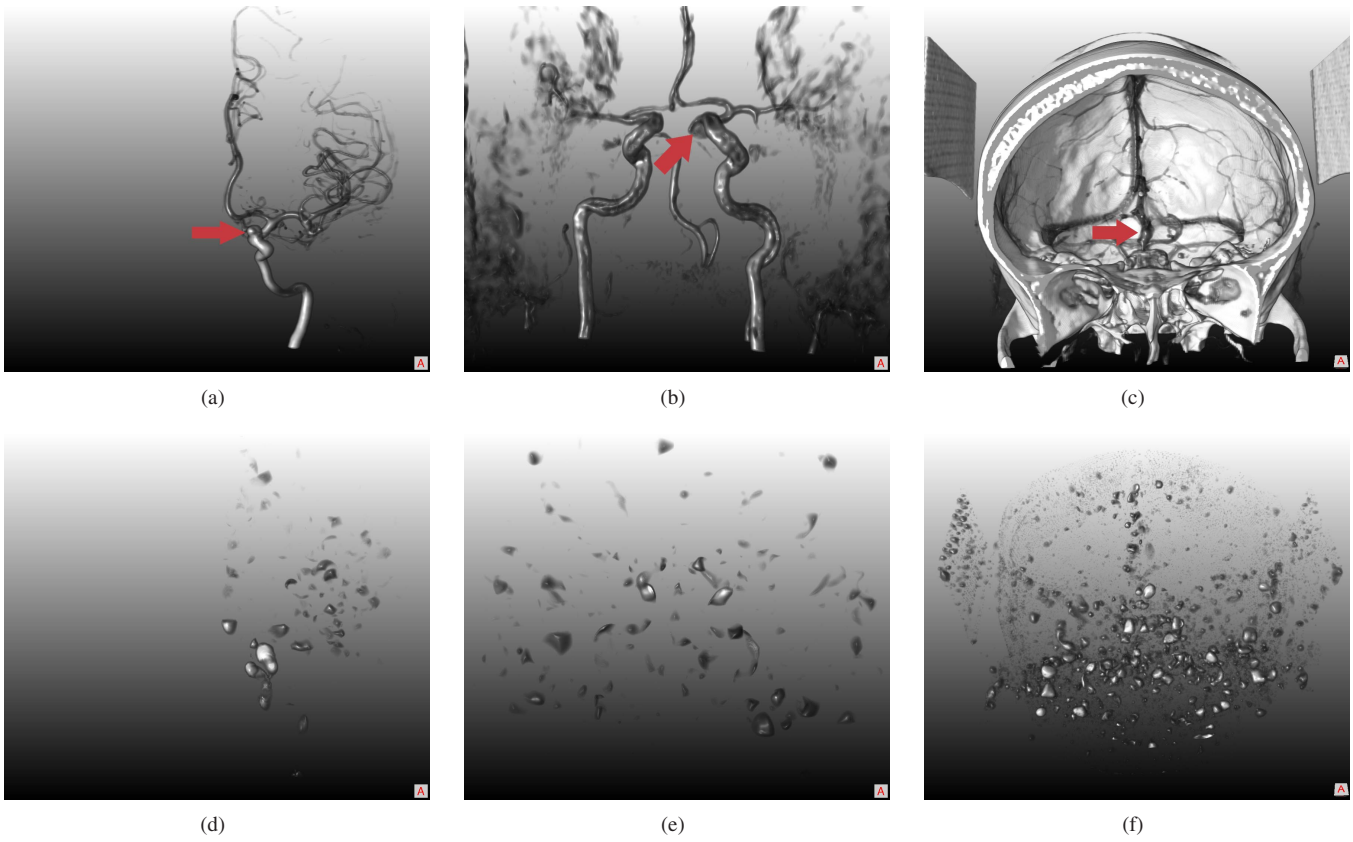

Fig. 1. Volume renderings of examples of (a) 3D-RA, (b) MRA and (c) CTA. The aneurysms are marked by arrows. The corresponding blobness-filtered volumes are shown in (d)-(f).

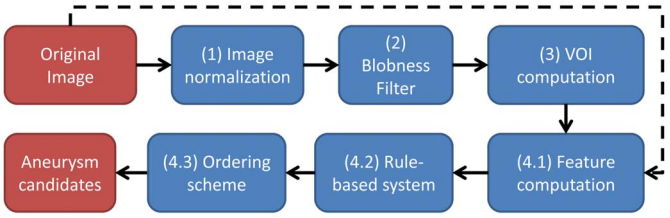

Fig. 2. Scheme of the proposed method.

Fig. 1(d)-1(f)). The filter is a generalization of the vesselness-filter aiming at enhancing n-dimensional vessel structures in m-dimensional medical images [8]. This approach assumes a spherical aneurysm shape. Although this is not always true, it still remains a good approximation for the vast majority of aneurysms. The filter is adjusted to find sphere-like structures with diameters between 2 mm and 10 mm. Larger structures are also found as (multiple) sub objects. Additionally, a vesselness filter is applied to the original image enhancing structures with a typical vessel diameter between 2 mm and 6 mm [8]. For the computation of the sphere-enhancing and vessel-enhancing CTA image, an image mask is created taking only voxels between 75 and 400 HU into account that represent contrast enhanced vessel structures.

Step 3 involves a clustering done by extraction of local maxima of the filtered image. It is desirable to simultaneously define a VOI around each maximum that represents the reach of each maximum. We use a modified k-means clustering to define VOI on the filtered image. It is not possible to use the standard k-means clustering algorithm for our purpose as the number of clusters is not known in advance. Therefore, we incorporate the minimum distance between clusters into the algorithm. Similar methods only extract the local maxima and then use segmentation algorithms to determine VOI around the maxima [4], [7].

The highest 25 % values of the remaining voxels that have a value $> t$, denoted as v_i, are assigned to the VOI V_j that has the smallest distance with j satisfying:

$$\arg\min_j d(v_i, V_j),\ j = 1, \ldots, n. \tag{1}$$

n is the amount of VOI. If this distance is larger than d_{min} or no VOI exists, a new VOI is created consisting only of this voxel. The distance between a VOI and a voxel is measured by computing the Euclidian distance between the voxel coordinates and the VOI center.

13 distinct features are computed on each VOI in step 4.1 (on the original image):

- average, minimum and maximum intensity (i_{avg}, i_{min}, i_{max}),
- average, minimum and maximum blobness (b_{avg}, b_{min}, b_{max}),
- average, minimum and maximum vesselness (v_{avg}, v_{min}, v_{max}),
- distances of the VOI to the image boundary (d_x, d_y, d_z),

- volume (Vol).

VOI are excluded by a rule-based system to reduce the amount of FP (step 4.2). This is done depending on their modality. In all modalities they are excluded if they are near the image boundary: $d_x < 0.2 \cdot s_{ix}$ with $d_x = \min(p(v_{ix}), p(v_{ix}) - s_{ix})$, where $p(v_{ix})$ is the x-coordinate of the VOI center and s_{ix} is the size of the image in x direction. y and z directions are defined analogous.

If CTA is the image modality, each VOI having an average intensity between 75 and 400 HU is further taken into account.

For MRA, VOI are analyzed based on a symmetry similarity measure. This aims to exploit the symmetry of the human vasculature. Symmetries appear commonly in the vasculature, whereas abnormalities are usually not symmetric. Symmetric aneurysms are possible, but it is very unlikely that they share the same features. The symmetry similarity is computed as follows: Each VOI is compared with each other VOI. If the VOI are symmetric (within a specified tolerance), the distance in feature space is computed (Equation 2). If this distance is below a threshold $\theta = 1.0$, both VOI are excluded. The distance is defined as follows:

$$d(V_1, V_2) = \sqrt{d_i^2 + d_b^2 + d_v^2}, \tag{2}$$

where

$$d_i = w_2 \cdot \left(\frac{i_{avg}(V_1) - i_{avg}(V_2)}{i_{avg}(V_2)} + \frac{i_{max}(V_1) - i_{max}(V_2)}{i_{max}(V_2)} \right),$$
$$d_b = w_1 \cdot \left(\frac{b_{avg}(V_1) - b_{avg}(V_2)}{b_{avg}(V_2)} + \frac{b_{max}(V_1) - b_{max}(V_2)}{b_{max}(V_2)} \right),$$
$$d_v = w_3 \cdot \left(\frac{v_{avg}(V_1) - v_{avg}(V_2)}{v_{avg}(V_2)} + \frac{v_{max}(V_1) - v_{max}(V_2)}{v_{max}(V_2)} \right).$$

$w_i \in W, i = 1, 2, 3$ are weighting factors set to $W = \{2, 1, 1\}$ to emphasize the blobness. For CTA, this symmetry similarity is not suitable as many VOI appear that do not consist of vessels and therefore the requirement is no longer fulfilled.

The VOI are sorted according to a chosen feature (step 4.3). VOI containing the n highest feature values are taken as aneurysm candidates, where n depends on the modality and is subject for evaluation experiments. All other VOI are interpreted as FP and are excluded from further consideration. The remaining VOI are taken as final aneurysm candidates.

III. Results

Our method was tested on 30 3D-RA, 20 MRA and 15 CTA patient data sets incorporating 27, 16 and 19 aneurysms, respectively. We note that no bone-subtraction CTA images were available and we used normal CTA images. In these images, intensities for contrast enhanced vessels and bones lie within the same range. 13 of the MRA data sets were acquired with the time-of-flight protocol while 7 were contrast enhanced MRA. The maximum size of the aneurysms was between 1.5 mm and 32 mm. The 3D-RA data sets had an isotropic voxel size with a resolution of 0.54 mm. The MRA data sets were resampled to an isotropic pixel size between 0.43 mm and 0.78 mm. The CTA data sets were resampled to an isotropic pixel size of 0.7 mm.

TABLE I
FEATURES AND THEIR DISCRIMINATORY POWER WITH RESPECT TO TP AND FP. THE BEST AUC VALUE FOR EACH MODALITY IS PRINTED BOLD.

feature	3D-RA	MRA	CTA
Vol	**0.81**	0.64	0.66
i_{avg}	0.64	0.56	0.58
i_{min}	0.62	0.43	0.40
i_{max}	0.66	0.55	0.29
b_{avg}	0.78	**0.67**	**0.69**
b_{min}	0.64	0.43	0.19
b_{max}	0.79	0.65	0.66
v_{avg}	0.72	0.60	0.67
v_{min}	0.68	0.48	0.36
v_{max}	0.73	0.59	0.64

The main difference between the image modalities is the amount of visible vessels. In 3D-RA the contrast agent is injected into one of the four major arteries and only this vessel and their successors are visible. In case of MRA and CTA, the whole cerebral vasculature is present in the data set leading to a larger amount of visible vessels. Also, the contrast between vessel and background tissue is higher in 3D-RA while in MRA data sets some artifacts are visible. Due to these facts, the detection of aneurysms is more challenging in CTA and MRA than in 3D-RA.

The ground truth was given by a neuroradiologist who had access to the clinical report. All experiments have been performed on each modality separately.

The parameter values for the clustering step were found empirically. Voxels with $t < 20$ % of the maximal blobness value were excluded if 3D-RA or MRA was used; for CTA, the value was $t < 5$ % of the maximal blobness value (Eq. 1). Based on experiments, we found that d_{min} =10 mm was a suitable value.

Experiments have been conducted to evaluate the quality of the different features as criterion for aneurysm detection. The VOI with n highest feature values are taken as aneurysm candidates, all others are assumed to be FP. The quality is measured by a free-response operator characteristic (FROC, Fig. 3(a)-3(c)), more specific by the area under curve (AUC). The AUC values are summarized in Table I. For 3D-RA, the volume, maximum blobness and average blobness value were the three features leading to the best AUC value. For MRA, average blobness, maximum blobness and volume were the best features and for CTA, average blobness, average vesselness and maximum blobness were the features leading to the best results. Consequently, VOI having the $n = 4$ highest respective feature values for 3D-RA, $n = 11$ for MRA and $n = 31$ for CTA are taken as aneurysm candidates as they lead to the best quality.

In summary, we measured 96.3 % sensitivity with an average rate of 2.6 FP per data set (FP/DS) for 3D-RA, 93.8 % sensitivity with an average rate of 8.0 FP/DS for MRA and

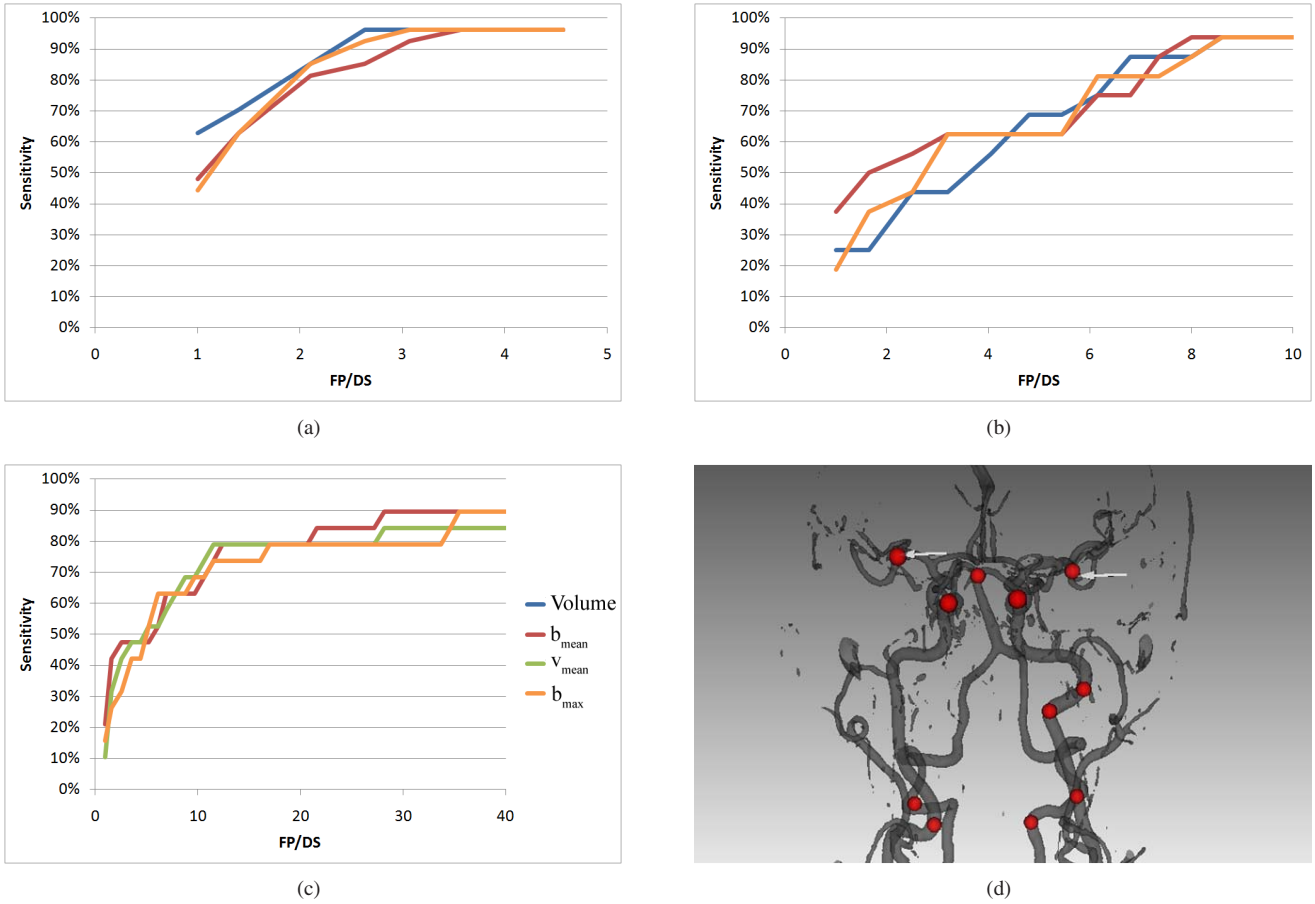

Fig. 3. FROC of (a) 3D-RA, (b) MRA and (c) CTA. Only the best three features are shown for better overview. Note that the scale of the x-axis differs in all three figures. b_{avg} = average blobness, b_{max} = maximum blobness, v_{avg} = average vesselness. (d) An example of the result visualization. The aneurysms are indicated by arrows.

89.5 % sensitivity with an average rate of 20.8 FP/DS for CTA. These results were measured using the features having the best discriminatory power.

Overall, only 4 of 62 aneurysms remained undetected by our method. These were two hardly visible aneurysms in CTA due to vicinity to bone and vicinity to a large aneurysm, one very small aneurysm in MRA and one aneurysm in 3D-RA.

We reached our goal of applying one algorithm to three angiographic modalities. It is difficult to compare our method to similar methods [4], [6] as we focused on different aspects, require no segmentation and do no statistical classification. Despite our restrictions, our quality is similar to other publications in case of the clinically relevant MRA where almost all other algorithms are specialized for. The high FP rates on CTA data sets can be explained by the considerably larger image information that is present in CTA.

IV. Conclusion

We proposed an algorithm for the automatic detection of cerebral aneurysms. We find sphere-like regions by a multi-scale enhancement filtering based on an eigenvalue analysis of the Hessian matrix. VOI are found by a modified k-means clustering on the filtered image. 13 features are computed on the VOI and each is used as a simple thresholding classifier. The features leading to the best quality were volume, maximum blobness and mean blobness for all modalities.

The algorithm is the first to work with 3D-RA, MRA and CTA data sets. Furthermore, the algorithm is the first to work on native CTA data sets without bone subtraction. In contrast to similar approaches, we do not need a vessel segmentation. We evaluated our algorithm with 65 angiographic data sets. Only 4 aneurysms are missed by our approach. The sensitivity is dependent on the modality. We reach at least 90 % sensitivity with an average FP rate between 2.6 and 20.8 per data set.

For the future, we plan to lower the amount of false positives by including high-level knowledge like location information. Additionally, we plan to test our algorithm with more data sets.

Acknowledgment

We thank Uta Preim for fruitful discussion. She is with the Heart Center, University of Leipzig.

References

[1] J. M. Wardlaw and et al., “The detection and management of unruptured intracranial aneurysms.” *Brain*, vol. 123, no. 2, pp. 205–21, Feb. 2000.
[2] J. van Gijn and et al., “Subarachnoid haemorrhage.” *Lancet*, vol. 369, no. 9558, pp. 306–18, Jan. 2007.

[3] J. I. Suarez and et al., "Aneurysmal subarachnoid hemorrhage." *The New England journal of medicine*, vol. 354, no. 4, pp. 387–96, Jan. 2006.
[4] H. Arimura and et al., "Computerized detection of intracranial aneurysms for three-dimensional MR angiography: Feature extraction of small protrusions based on a shape-based difference imaging technique," *Medical physics*, vol. 33, no. 2, p. 394, 2006.
[5] S. Kobashi and et al., "Diagnosis of Intracranial Aneurysms in MRA Images with Case-Based Reasoning," *IEICE Transactions on Information and Systems*, vol. 89D, no. 1, pp. 340–350, 2006.
[6] A. Lauric and et al., "Automated detection of intracranial aneurysms based on parent vessel 3D analysis," *Medical Image Analysis*, vol. 14, no. 2, pp. 149–159, 2010.
[7] X. Yang and et al., "Computer-Aided Detection of Intracranial Aneurysms in MR Angiography." *Journal of digital imaging*, 2009.
[8] A. Frangi and et al., "Multiscale vessel enhancement filtering," in *Medical Image Computing and Computer-Assisted Intervention (MICCAI)*, 1998, pp. 130–137.

View publication stats